16th World Conference on Earthquake, 16WCEE 2017

Santiago Chile, January 9th to 13th 2017

Paper N° 1107 (Abstract ID)

Registration Code: S-K1463060534

STRENGTHENING OF MASONRY STRUCTURES WITH CEMENTITIOUS MATRIX COMPOSITE

V. Alecci[(1)], L. Rovero[(2)], G. Stipo[(3)], M. De Stefano[(4)]

[(1)] *Assistant Professor, University of Florence (Italy), valerio.alecci@unifi.it*
[(2)] *Assistant Professor, University of Florence (Italy), luisa.rovero@unifi.it*
[(3)] *PhDoctor, University of Florence (Italy), gianfranco.stipo@unifi.it*
[(4)] *Full Professor, University of Florence (Italy), mario.destefano@unifi.it*

Abstract

Seismic risk mitigation of historical masonry buildings comprises a challenge of growing relevance for both scientific research and engineering practice. Especially for buildings of high historical value, retrofitting techniques must be compliant with the basic principles of conservation, i.e. non-invasiveness, reversibility and compatibility.

In this perspective, fabric-reinforced cementitious matrices (FRCMs) are becoming increasingly suitable for strengthening of historic masonry constructions in seismic areas, as an alternative to Fiber Reinforced Polymers (FRPs) .

Cementitious matrix composites are easy to apply, have a resistance against high temperatures comparable with the support, can be applied to damp surfaces, and have excellent physical–chemical compatibility with the masonry substrates. Furthermore, if compared with FRP composites, FRCM composites permit higher vapor permeability, lower costs, and a complete reversibility of the installation. These qualities assume a major relevance for ancient masonries retrofitting, where both the seismic safety and the conservation criteria need to be met.

Although FRCM systems have attracted growing interest in the strengthening of masonry structures, only few experimental studies are still available.

In this paper, experimental data from an extensive testing program are presented in order to better understand mechanical behaviour of PBO-FRCM composite and to properly design seismic reinforcements. Specifically, bond performance between bricks masonry and PBO-FRCM composite are investigated through both beam tests and double shear tests. Mechanical behaviour of masonry arches reinforced at intrados and extrados by PBO-FRCM composite are investigated through experimental test on arch models. In particular, six masonry arch models (1:2 scale), both un-strengthened and strengthened at extrados or intrados and subjected to a vertical force, are comprised in the experimental program.

Results in terms of load-carrying capacity, post peak behavior and failure mechanism were reported and commented.

The laboratory data demonstrated that PBO-FRCM composite is an effective solution for the strengthening of masonry members, being able to improve their load-carrying capacity as well as their ductility capacity (specific requirement of the current seismic codes).

Keywords: masonry, composite material, fabrics/textiles; fiber/matrix bond; arch; experimental test

1. Introduction

Historical masonry buildings, constituting a large part of the world architectural heritage, often include arches and vaults of high architectural value. The maintenance of the safety and usability of these structures is a challenging task for architects and engineers because repairing and/or strengthening interventions need to meet both the seismic safety and the conservation criteria.

Nowadays, traditional strengthening techniques of arches and vaults, such as the application of steel profiles at the arches intrados, the insertion of steel rebars, the injection of cementitious mortar and the application of reinforced concrete hoods, are considered unsuitable due to their aesthetic impact and, mainly, to the not desidable addition of extra weight and stiffness to the structure, in case of seismic actions.

The recent wide development of composite materials for constructions allowed to overcome these disadvantages. FRP (Fiber Reinforced Polymer) strips, applied at intrados or extrados of vaulted structures, demonstrated able to improve their structural performance, both in terms of load carrying capacity and ductility [1-4].

More recently, the scientific community raised the issue of the scarce physical-chemical compatibility of FRP composites with the masonry substrate, particularly in the case of historical and artistic constructions for which the compatibility with the original material is often a specific requirement. For this reason, innovative composites made of a fabric embedded in a cement-based mortar (FRCM, Fabric Reinforced Cementitious Matrix) have been proposed as an alternative to FRP composites, expecially for strengthening historical and monumental masonry constructions [5-9].

The use of FRCM composites for strengthening masonry members is still to an early stage and few experimental data are available in the literature.

In this perspective, the present paper experimentally investigates the structural behavior of masonry arches strengthened by applying, at the whole intrados or extrados surface, a polybenzoxazole (PBO) fabric reinforced cementitious mortar (FRCM) composite sheet. Six masonry arch models (1:2 scale) subjected to a vertical force were tested. The experimental study also involved the mechanical characterization of masonry and composites and their components. Furthermore, the bond capacity between composite and brick was investigated by beam tests and double shear tests.

2. Experimental investigation

The experimental investigation was carried out on un-strengthened and both extrados and intrados strengthened masonry arch models (1:2 scale). A first stage of the experimental campaign was devoted to the mechanical characterization of the masonry and its constituent materials, cement-lime mortar and bricks. Beam tests and double shear tests were performed to investigate the bond performances of the two composites and tension and compression tests were carried out on PBO textile and cement-based matrix respectively.

2.1 Mechanical characterization of masonry

Masonry used for the construction of the arch models was mechanically characterized by compression tests. Furthermore, the mechanical properties of the masonry constituent materials, cement-lime mortar and bricks, were also determined before their assemblage. In particular, mechanical characterization of cement-lime mortar was performed according to [10] and reported in Table 1. Mechanical characterization of bricks was performed according to UNI EN 772-1 [11]. In Table 1, the average values of compressive and flexural strength of tested bricks are reported.

In a second step, these constituent materials were assembled for creating 6 masonry prisms, 1:2 scaled, subsequently subjected to uniaxial compression tests. In particular, the masonry prism texture was constituted by 6 mortar layers, 5 mm thick, and 14 bricks, 21 x 46 x 95 mm^3 in size, obtained by cutting common bricks produced by S. Marco Laterizi Company. In Table 1, the average values of compressive strength, compressive elastic modulus and ultimate strain are reported.

Table 1 - Results of uniaxial compression tests and three points bending tests on bricks, cement-lime mortar, and masonry (the standard deviation and the coefficient of variation are reported in parentheses).

Specimen	Failure compressive strain	Compressive strength (MPa)	Compressive Young modulus (MPa)	Flexural Tensile strength (MPa)
Cement-lime Mortar	/	3.22 (0.31; 9.72)	727.7 (69.82; 9.59)	1.49 (0.025;1.68)
Brick	/	24.08 (2.73; 11.37)	2701,81 (585.05; 21.65)	5.60 (0.58; 10.44)
Masonry	0.0076 (0,002; 17.66)	8.53 (1.29; 13.95)	1753.7 (282.52; 16.11)	/

2.2 Mechanical characterization of the FRCM composite

The FRCM composite used in the present experimental study is made of a polybenzoxazole (PBO) bidirectional balanced textile consisting of 14 mm spaced rovings, with a nominal thickness in both fiber directions equal to 0.014 mm. The free space between rovings is roughly 11 mm. Warp and weft rovings are overlapped but not connected at the intersections. The matrix is constituted by a pozzolanic cement-based matrix.

Mechanical properties of the PBO-FRCM composite were firstly investigated thorough the mechanical characterization of the constituent materials, cementitious mortar matrix and PBO textile. Average values of experimental test results are reported in Table 2. PBO textile was characterized by direct tensile test according to [12]. The average values of mechanical properties of PBO textile are summarized in Table 3.

Table 2 - Results of uniaxial compression tests and three points bending tests on the cementitious matrix (the standard deviation and the coefficient of variation are reported in parentheses).

Component material	Compressive strength (MPa)	Compressive Young modulus (MPa)	Flexural tensile strength (MPa)
Ruregold MX	20.22 (2.12; 10.51)	2874.72 (458.38; 15.94)	6.15 (0.35;5.7)

Table 3 - Mechanical properties of textiles ([a] data experimentally determined in this study; [b] data provided by the manufacturer - Ruredil S.p.A., 2013).

Component material	Tensile strength (MPa)	Tensile strength per unit width (N/mm)	Tensile Young modulus (MPa)	Ultimate strain
PBO	3328[a]	46.59[a]	223382[a]	0.0149[a]

2.3 Bond capacity of the PBO-FRCM composite: beam test and double shear test

The characterization of the composite material used to strengthen the masonry arches was also performed in terms of bond capacity. In particular, beam tests were carried out on 12 specimens on which the FRCM composite was applied in order to investigate the bond capacity (Fdb), i.e. the maximum force that can be transferred to the masonry substrate. Each of the 12 tested specimens was made of two bricks connected by a metallic hinge on the compression side and by the FRCM composite sheet on the tension side. The composite sheet 95 mm width (the same width of the sheet applied to strengthen the masonry arches) was applied along the whole length of the specimen comprised between the two steel cylinder supports. The load was applied by a spherical hinge placed on a metallic plate and transferred to the specimen by two metallic cylinders. Each specimen was equipped with three displacement transducers (type CE cantilever): one of them was positioned on the metal hinge to measure the vertical displacement of the mid-span cross-section and two at the specimen ends to measure the displacement of the supports. In Table 4, test results in terms of maximum applied load F_{max} are reported.

Table 4 - Average values of beam-test results. (the standard deviation and the coefficient of variation are reported in parentheses).

Specimen code	Composite material	Composite sheet width (mm)	Maximum force F_{max} (N)
1-12F	FRCM	95	2378 (112.37; 4.72)

The failure of specimens was characterized by a textile-matrix slip occurred at the mid-span cross-section while cementitious matrix remained perfectly attached to the substrate. The bond capacity F_{db} of the composite material was obtained through the equilibrium between internal moment and the mid-span bending moment relative to the maximum applied force F_{max}. The tests provided an average bond capacity $F_{db,m}$ for the FRCM composite equal to 5096 N.

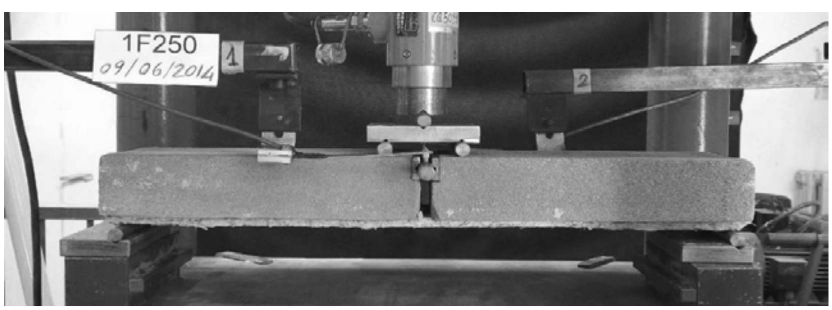

Fig. 1 – Beam test

Double shear tests were performed on 9 specimens, partitioned into 3 groups. Each group is constituted by 3 specimens and it is characterized by different bond lengths (150 mm, 200 mm and 250 mm), as reported in the left columns of Table 5.

For the specimens assemblage, the bricks were duly moistened and then a first layer of the cement matrix of about 3 mm thick was applied. Therefore, the PBO textiles were positioned on matrix layer and a second cementitious matrix layer was then applied, reaching a total thickness of about 6 mm. This procedure was carried out on both principal faces of each specimen. The specimens were tested using a properly designed apparatus consisting of a double steel frame where the two bricks connected by the composite sheets were positioned. The two metal frames are symmetrical with respect to the horizontal axis. Each metal frame consists of two 15 mm thickness steel plates connected by two threaded bars (20 mm in diameter) that firmly clamp the bricks. Global measures were acquired by linear variable differential transformer integrated in the testing machine with 1 mm of resolution.

The double shear test set up was designed so as to transfer the load from the bricks to the composite. This test set up permitted the overcoming of the typical problems related to the efficacy of the gripping systems. Furthermore, the symmetry of the test apparatus avoided misalignments in the load application.

Table 5 summarizes the experimental results in terms of bond length, maximum load and ductility factor. The ductility factor was determined as the ratio of the ultimate displacement (measured in correspondence of a load of the softening branch equal to the 80% of the peak load) to the displacement in correspondence of the peak load. The effective length of the strengthening composites is to be considered less than 150 mm.

All the tested specimens showed a failure mode characterized by a gradual loss of adhesion at the fiber/matrix interface. In particular, a considerable slip occurred at the fiber/matrix interface, after a first transversal cracking of the cement matrix in the middle of the specimen. This slip phenomenon is macroscopically observable in Fig. 1 where the failure area is properly magnified. For the tested specimens, the debonding of the reinforcement from the substrate never occurred, differently from the typical failure mode of FRP composite.

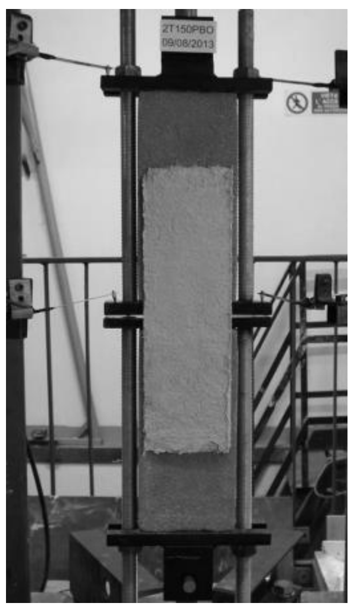

Fig. 2 – Double shear test

Table 5 - Results of bond tests on composites

Specimen code	Textile	Bond length (mm)	Maximum load (N)	Ductility factor
1T150PBO	PBO	150	3370	1.03
2T150PBO	PBO	150	3420	1.07
3T150PBO	PBO	150	3440	1.05
1T200PBO	PBO	200	3230	1.06
2T200PBO	PBO	200	3290	1.06
3T200PBO	PBO	200	3340	1.07
1T250PBO	PBO	250	3390	1.09
2T250PBO	PBO	250	3290	1.06
3T250PBO	PBO	250	3340	1.07

2.4 Arch testing

Experimental campaign addressed six 1:2 scaled masonry arches. Two specimens were tested in the unstrengthened configuration (specimens 1-US and 2-US) and four specimens were strengthened with PBO-FRCM composite, two at the extrados and two at the intrados (specimens 1-2/PeS and 1-2/PiS respectively).

Bricks were 95 × 46 × 21 mm3 sized with average thickness of the mortar layers of 5 mm, according to the scale of the arch models. The arches had a 1500 mm span, with 866 mm intrados radius, 961 mm extrados radius, 432.5 mm rise, and 95 × 95 mm2 cross section (width by thickness).

Each unstrengthened and strengthened arch was subjected to a vertical force, applied by using a displacement control device made of a screw jack controlled through a flywheel. The use of the displacement control device permitted to observe the whole loading history, up to the point of a conventional test-end corresponding to a residual strength equal to 80% of the peak load.

The load was applied at a quarter of the span (375 mm from the left abutment) using a squared steel plate 20 mm thick and it was measured through a load cell with a capacity of 10 kN (TCLP-10B tension/compression load cell). Vertical displacements were measured by means of two displacement transducers (type CE cantilever) positioned on the metallic plate. The transducers and the load cell were connected to a computer through an electronic control unit that directly displayed the load-displacement curve.

During the tests, observation of the specimens and analysis of the contemporary displayed load-displacement curve allowed to record cracks, stiffness variation, hinges formation, failure modes.

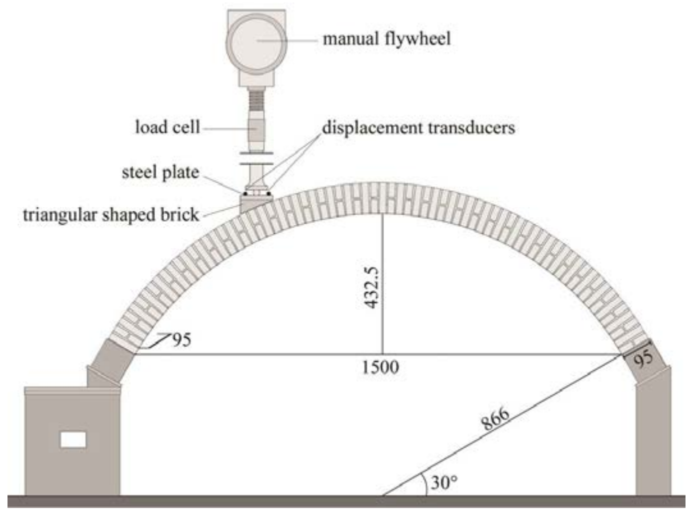

Fig. 3 – Test apparatus for the arch models

4. Test results

Test results are illustrated thorough load-displacement diagrams (Fig. 4) and reported in Table 6 for unstrengthened (US) arches and PBO-FRCM strengthened arches at intrados (PiS) and extrados (PeS).

The following structural parameters are identified: maximum load, stiffness, kinematic ductility and available kinematic ductility. Stiffness was determined in the linear range of the load–displacement curve, in order to avoid the influence of the non-linear start of the load path produced by the contact between load plate and specimen surface. Kinematic ductility (i.e. the capacity of the specimen to show large displacements after the linear elastic phase up to the maximum load) was calculated as the ratio of the displacement measured at the maximum load, to the displacement corresponding to the linear elastic limit of the load path; available kinematic ductility (i.e. the capacity of the specimen to show large displacements after the maximum load up to the ultimate load) was taken as the ratio of the ultimate displacement (displacement corresponding to the ultimate load, conventionally assumed to be equal to 80% of the maximum load) to the displacement at the maximum load.

The fifth column of the Table 6 shows the observed failure mode for each tested specimen.

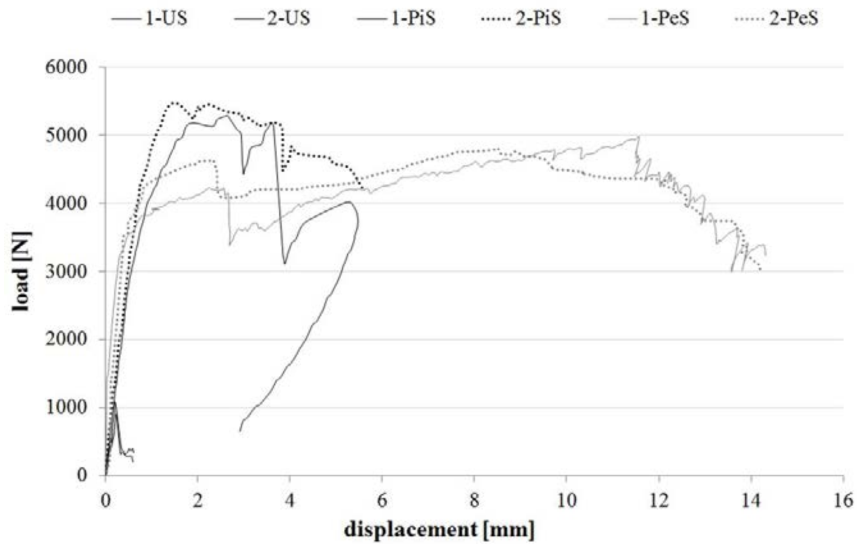

Fig. 4 – Load-displacement curves of the unstrengthened and PBO-FRCM strengthened arches (Us= unstrengthened; iS=intrados strengthened; eS= extrados strengthened).

The following structural parameters are identified: maximum load, stiffness, kinematic ductility and available kinematic ductility. Stiffness was determined in the linear range of the load–displacement curve, in order to avoid the influence of the non-linear start of the load path produced by the contact between load plate and specimen surface. Kinematic ductility (i.e. the capacity of the specimen to show large displacements after the linear elastic phase up to the maximum load) was calculated as the ratio of the displacement measured at the maximum load, to the displacement corresponding to the linear elastic limit of the load path; available kinematic ductility (i.e. the capacity of the specimen to show large displacements after the maximum load up to the ultimate load) was taken as the ratio of the ultimate displacement (displacement corresponding to the ultimate load, conventionally assumed to be equal to 80% of the maximum load) to the displacement at the maximum load.

The fifth column of the Table 6 shows the observed failure mode for each tested specimen.

Fig. 4 shows the load-displacement curve of the loaded cross section of the unstrengthened and both intrados and extrados PBO-FRCM strengthened arches. It can be noted the considerable contribution of PBO-FRCM material in increasing the maximum load and ductility (kinematic ductility as well as available kinematic ductility). The initial stiffness was similar in the unstrengthened and intrados strengthened arches while the extrados strengthened arches showed an higher stiffness. An important difference was observed comparing the effect of the strengthening at the intrados and extrados surfaces. In fact, the arches strengthened at the extrados exhibited a higher kinematic ductility than those strengthened at the intrados. On another hand, the maximum load didn’t show considerable variations.

Table 6 - Results of tests on unstrengthened and strengthened arches (Us= unstrengthened; PiS= PBO-FRCM intrados strengthened; PeS= PBO-FRCM extrados strengthened).

Specimen	**Maximum load (N)**	**Tangent stiffness (N/mm)**	**Kinematic ductility**	**Available kinematic ductility**	**Failure mode**
1-US	910	7179	1.85	1.10	Hinges mechanism
2-US	1066	6197	1.11	1.18	Hinges mechanism
1-PiS	5280	5891	2.77	1.42	Debonding+masonry crushing
2-PiS	5672	5510	3.64	2.12	Debonding+masonry crushing
1-PeS	4968	16221	20.32	1.11	Shear sliding
2-PeS	4813	9946	19.46	1.51	Shear sliding

Results reported in Table 6 confirm the effectiveness of PBO-FRCM composite in increasing the maximum load (by approximately 400% for extrados strengthening and 480% for the intrados one) and the ductility. In particular, the kinematic ductility resulted considerably increased in case of extrados application (approximately 13 times the value of the unstrengthened arches) with respect to the case of intrados application (2 times the value of the unstrengthened arches).

As was expected, the unstrengthened arches exhibited a collapse mechanism with four alternate (intrados/extrados) hinges (Fig. 5). The first hinge occurred at the arch extrados at the loaded cross section and the second hinge at the intrados, in a symmetric position with respect to the previous one. The third and fourth hinge occurred approximately on the left and right abutment respectively. In Fig. 5, the position and order of formation of the hinges on the unstrengthened arches are represented.

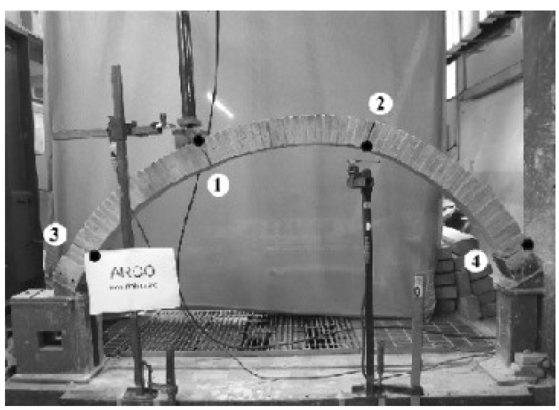

Fig. 5 – Sequence of hinges formation on the unstrengthened arches

The application of PBO-FRCM strengthening composite at the extrados or intrados of the arches, modified the collapse mechanism. Concerning the extrados application (Fig. 6) it was observed that the onset of the hinge formation on the loaded cross-section, revealed by thin cracks appeared on the mortar joint, coincided with the linear elastic phase limit. A further increase of the load produced the opening of the first hinge. At the same time, a slight debonding at the composite-to-masonry interface was observed, also revealed by a sudden load reduction at constant displacement rate. The presence of PBO-FRCM composite at the extrados partially prevented the opening of the relative hinges so, in this case, only superficial cracks of the cementitious matrix were observed approximately where second and third hinges occurred in the unstrengthened arches. In this phase the load slightly increased reaching a peak load of 4968 N and 4813 N for 1-PeS and 2-PeS arches respectively.

After, additional cracks occurred on the matrix allowing a large displacements up to the arch collapse, due – after many warnings – to shear sliding at the right abutment.

Fig. 6 – Failure details of PBO-FRCM extrados strengthened arches: a) hinge formation on the loaded cross section; b) superficial cracking of the cementitious matrix; c) shear sliding at the right abutment.

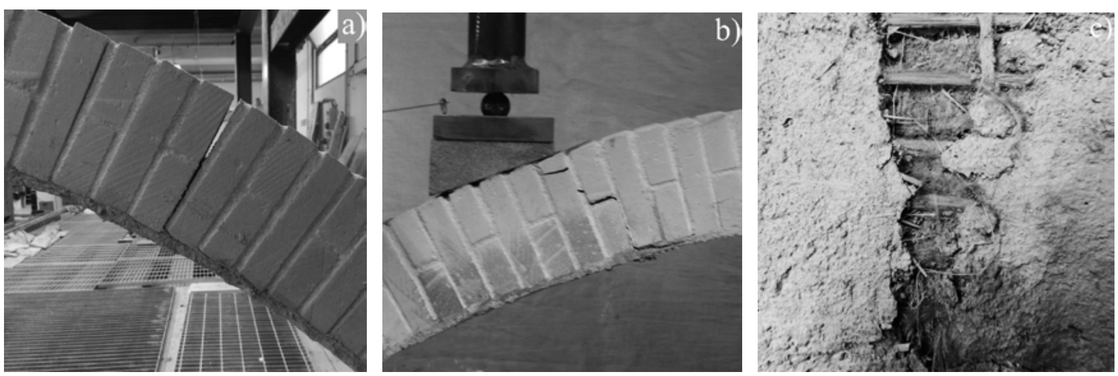

Fig. 7 – Failure details of PBO-FRCM intrados strengthened arches: a) first hinge; b) masonry crushing; c)debonding at the textile-mortar interface.

The intrados PBO-FRCM strengthened arches (Fig.7) exhibited a different failure mode involving the the debonding at the PBO textile-mortar interface and the crisis of the masonry near the loaded cross section. More precisely, both in case of 1-PiS and 2-PiS specimens, the linear elastic limit coincided with the formation of a first crack where second hinge occurred in the unstrengthened arches. In the case of intrados strengthening, in fact, the presence of the PBO-FRCM material prevented the opening of hinge on the loaded cross section. With the increase of the load, the crack opened and a first hinge formed. After this phase, arches quickly reached their maximum load capacity. Subsequently, superficial cracks of the cementitious matrix and a crack involving mortar joints and bricks at the loaded cross section were observed. The post-peak phase was characterized by an increasing of the masonry crushing and of the debonding phenomenon at the textile-mortar interface. Many warnings were provided before failure. At the end of the test, the PBO-FRCM composite remained fixed to the substrate but an evident debonding at the PBO textile-mortar interface resulted.

5. Conclusions

The present experimental investigation covers the structural performance of masonry arches strengthened both at intrados and at extrados by using a polybenzoxazole (PBO) fabric reinforced cementitious mortar (FRCM). More precisely, the experimental work involved the test of six masonry arch models (1:2 scale) subjected to a vertical force. The experimental study also concerned the mechanical characterization of masonry and composites and the investigation – through beam tests and double shear tests– on the bond capacity between composite and brick.

Concerning the arch testing, the principal mechanical parameters (load-carrying capacity, stiffness and ductility) were determined and failure mechanisms were accurately described and interpreted.

The following conclusions can be deduced from the experimental results:

- PBO-FRCM composite demonstrated effective in increasing the maximum load (more than 400% of the values of the unstrengthened arch) both in the case of extrados and intrados application.

- In terms of ductility, a difference between intrados and extrados application of PBO-FRCM composite was observed. In particular, kinematic ductility resulted approximately 13 times the value of the unstrengthened arches in the case of extrados application while 2 times the value of the unstrengthened in the case of intrados application.

The laboratory data demonstrated that PBO-FRCM composite is an effective solution for the strengthening of masonry members, being able to improve their load-carrying capacity as well as their ductility capacity (specific requirement of the current seismic codes). Furthermore, the high physical-chemical compatibility with the masonry substrate makes this innovative composite particularly useful in the case of strengthening interventions on historical and artistic buildings for which the compatibility with the original substrate is often a specific requirement.

5. References

[1] Rovero L, Focacci F, Stipo G (2013): Structural behavior of arch models strengthened using FRP strips of different lengths. *J Compos Constr*, **17** (2), 249–258.

[2] Briccoli Bati S, Rovero L, Tonietti U (2007): Strengthening of masonry arches with composite materials. *J Compos Mater*, **11** (1), 33-42.

[3] Briccoli Bati, S, Rovero, L (2008). Towards a methodology for estimating strength and collapse mechanism in masonry arches strengthened with fibre reinforced polymer applied on external surfaces. Materials and Structures, 41(7), 1291-1306.

[4] Rotunno T, Rovero L, Tonietti U, Briccoli Bati S (2014). Experimental study of bond behavior of CFRP-to-brick joints. Journal of Composites for Construction, 19(3), 04014063

[5] Prota A, Marcari G, Fabbrocino G, Manfredi G, Aldea C (2006): Experimental In-Plane Behavior of Tuff Masonry Strengthened with Cementitious Matrix–Grid Composites. *J Compos Constr*, **10** (3), 223-233.

[6] Carbone I, De Felice G (2009): Debonding of C-FRCM composite on masonry support. *9th International Conference on Protection of Historical Buildings (PROHITECH 09)*, Rome, Italy.

[7] Alecci, V., De Stefano, M., Luciano, R., Rovero, L., & Stipo, G. (2015). Experimental Investigation on Bond Behavior of Cement-Matrix–Based Composites for Strengthening of Masonry Structures. Journal of Composites for Construction, 20(1), 04015041.

[8] Garmendia L, Larrinaga P, San-Mateos R, San-José JT (2015): Strengthening masonry vaults with organic and inorganic composites: an experimental approach. *Materials & Design*, **85**, 102–114.

[9] D'Ambrisi A, Focacci F, Luciano R, Alecci V, De Stefano M (2015): Carbon-FRCM materials for structural upgrade of masonry arch road bridges. *Compos: Part B Eng*, DOI:10.1016/j.compositesb.2015.01.024.

[10] European Standard UNI EN 1015-11 (2007): Methods of test for mortar for masonry - Determination of flexural and compressive strength of hardened mortar.

[11] European Standard UNI EN 772-1 (2011): Methods of test for masonry units - Determination of compressive strength.

[12] ASTM D5034 (2013): American Society for Testing and Materials. Standard Test Method for Breaking Strength and Elongation of Textile Fabrics (Grab Test).